Chapter 11
Applications of X-Ray Nanochemistry in Sensing, Radiolysis, and Environmental Research

Good wine makes good conversation; Good people make good countries.

11.1 Introduction

X-ray nanochemistry may influence our life and surroundings in ways more than medical imaging and cancer treatment. Many of the basic and applicable principles are interconnected. For example, in the previous three chapters in Part IV of this book, DNA strand breaks, tumor destruction, and catalysis are closely connected to physical or chemical enhancement discussed in Part II, which are directly dependent on the nanomaterials and methods of detection described in Chaps. 6 and 7. The reverse is also true. The applications may provide useful feedback to and can even expand fundamental aspects of X-ray nanochemistry. For instance, damage to biomolecules and cells as discussed in Chaps. 8 and 9 may provide valuable feedback to biological enhancement described in Chap. 4; the photocatalysis described in Chap. 10 can help improve the understanding of chemical enhancement or type 3 physical enhancements described in Chaps. 2 and 3. In this chapter, three potential application areas are discussed, which are radiolysis, sensing, and environmental remediation. Each of these three areas is a stand-alone topic and is part of X-ray nanochemistry.

Radiolysis has dominated the landscape of radiation chemistry prior to using nanomaterials in an elaborate and comprehensive fashion to enhance the effectiveness of X-ray irradiation. In the past, nanoparticles were used either unknowingly, or knowingly but with relatively simple surface chemistry and without the enhancement described in Chaps. 2, 3, 4, and 5. With the assistance of X-ray nanochemistry, radiolysis may be greatly expanded in the future. As it is shown in this book, adding nanomaterials to samples under X-ray irradiation not only increases X-ray absorption and creates physical enhancement including additional UV emission, but also promotes catalysis that significantly increases the yield of radiolysis. Studies of radiolysis involving nanomaterials and molecules of various sizes have been reported in the literature. Some of the molecules have been discussed in the other chapters. Here, the emphasis is placed on the decomposition of large organic molecules.

T. Guo, *X-ray Nanochemistry*, Nanostructure Science and Technology,
https://doi.org/10.1007/978-3-319-78004-7_11

Many of the results reported to date employ γ-rays. The results obtained with γ-rays are often improved when X-rays are used due to increased absorption cross-sections of X-rays interacting with the chemicals involved, although the purpose of research may be completely changed. For example, hydrogen production by zirconia nanoparticles was studied by LaVerne et al. [1] for nuclear energy application purposes. However, there is no apparent immediate and practical value of using X-rays to produce hydrogen gas. The literature on studying radiolysis with γ-rays is reviewed in this section because the same principles are applicable to X-ray radiolysis; often the same study performed with γ-rays in the past can be done with X-rays to achieve better results without using expensive and often cost-prohibitive γ-ray sources.

Besides radiolysis, detection of ionizing radiation such as X-rays with nanomaterials can be important in protecting professionals as well as consumers, such as those who are sensitive to effects of ionizing radiation. Currently, there are many types of commercially available radiation sensors, but none of them uses X-ray nanochemistry technologies. The existing enhancement technologies using nanomaterials are still too immature to support sensitive and inexpensive detection of ionizing radiation, including X-rays. Besides recording radiation dosage, sensing can also be performed in the form of imaging by detecting certain materials at certain locations, including those at hidden or difficult to see or reach places. X-ray nanochemistry can be used in remote sensing, and its spatial resolution can be high, of the order of a few nanometers, as demonstrated by Guo et al. [2]. The publication showed that it was possible to probe the distance between two nanoparticles with nanometer spatial resolutions in hidden places. All these materials are covered in Sect. 11.4.

In a third application area to be discussed in this chapter, environmental remediation is described as a benefit from radiolysis of environmentally detrimental chemicals. Environmental research can also take advantage of chemical or physical enhancement as defined in X-ray nanochemistry so that X-ray or γ-ray energy can be converted to local chemical energies to breakdown the most persistent and toxic chemicals in the environment. In Sect. 11.5, published results are discussed to highlight this potential. In the future, these results can be further improved so that decomposition of these environmentally unfriendly chemicals can happen at much higher efficiencies and lower costs.

In this chapter, the published works in these three areas are reviewed and discussed. In addition, basic principles related to these three areas are also briefly discussed in Sect. 11.2 to give readers a more complete survey of the literature in these areas.

11.2 Basic Principles

This section deals with principles that govern the three areas of applications of X-ray nanochemistry discussed in the rest of the chapter. These principles are not the enhancement principles described in Part II. Radiolysis without nanomaterials and

nanomaterial-assisted radiolysis are discussed first. For sensing, both nanomaterial-assisted sensing and new methodologies involving nanomaterials and X-rays are given. No formal theory has been developed in the area of environmental remediation using X-ray nanochemistry.

11.2.1 Radiolysis

Radiolysis studies reactions that decompose chemicals under irradiation of ionizing radiation. A typical radiolytic reaction is decomposition of water, which has been extensively researched. Several review articles as well as book chapters, e.g., those in Farhataziz et al. [3], are written on this topic. As a result, radiolysis of water, a critical process to understanding many other important concepts such as chemical enhancement, is only briefly reviewed here. This is not the only place in this book where radiolysis of water is mentioned. Chapter 3 also briefly discusses irradiation of water with X-rays. The emphasis in Chap. 3 is placed on the generation of reactive oxygen species. The emphasis of this section is placed on the decomposition of solute molecules dissolved in water, especially in the presence of nanomaterials. Synthesis of nanomaterials under X-ray irradiation is not covered here.

11.2.1.1 Radiolysis of Water (by X-Rays)

X-rays interact with water to produce many reactive species. As stated in Chaps. 2 and 3, X-rays with energies between 10 and 1000 keV interact with water mainly through Compton scattering, which produces lower-energy X-ray photons and electrons, with most of the electrons having kinetic energy at approximately 2 keV and a small amount at 25 keV. The electrons and lower-energy X-ray photons then interact with water molecules to produce radicals including solvated electrons, hydrogen atoms, hydroxyl and superoxide radicals, perhydroxyl radicals, as well as the closed-shell molecule hydrogen peroxide.

The yield of these species changes as a function of time after their generation. For pulsed radiolysis using X-rays or electrons as the radiation source, yields are measured in G values, which are the number of a species produced per 100 eV of absorbed energy. Table 11.1 lists the G values of several of the most popular reactive oxygen species, as well as solvated electrons. These are the G values at 1 ps after

Table 11.1 Pulsed and steady state G values of radiolysis of water for low linear energy transfer (LET) radiation such as X-rays

	e^- (aq)	•H	H_2	•OH	$•HO_2$	H_2O_2
Pulsed (at 1 ps)	4.8	0.62	0.15	5.7		
Steady state	2.7	0.55	0.45	2.8	0.026	0.7

The values are adapted from Farhataziz et al. [3]

irradiation of water with a pulsed radiation source. For steady state, which means the products reach a steady state, the G values are also given in Table 11.1.

These are the yield of the species without any additives. Adding nanomaterials into the samples may significantly influence the generation mechanisms of these species. Currently there are many, albeit inconsistent, reports with respect to the dependency of generation of reactive oxygen species on nanomaterials. Further, the measurements may be affected by chemical enhancement, including anti-enhancement. The results reported in this area in recent years are briefly summarized in Sect. 11.3.

11.2.1.2 Radiolysis of Molecules Other than Water

X-ray or ionizing radiation radiolysis of molecules other than water without the use of nanomaterials has also been studied for a long time. Some of the processes involve the reactive species discussed in the previous subsection. There are many examples using reactive oxygen species to oxidize or reduce chemicals that lead to decomposition of chemicals. These reactions can be complex. For example, DNA strand breaks are complex reactions, usually starting with hydrogen abstraction or hydroxylation. CO_2 decomposition in water has also been widely reported. For example, the mechanism provided by Harteck et al. [4] is shown in reaction Eqs. 11.1, 11.2, 11.3, 11.4, 11.5, 11.6 and 11.7. The number of reactions was later expanded to include many more species in the theoretical modeling presented by Kummler et al. [5]. When catalytic reactions are possible, reaction mechanisms are much more complicated, as shown in Sect. 10.2.1. Again, most of the reported works to date are done with γ-rays, although it is reasonable to assume that when X-rays are employed, the yield of decomposition measured in G values will be higher. The dominant choice of using γ-rays in the past was mainly because of the connections to nuclear industry and partially due to interstellar research. With X-rays, the goal of research can be expanded to exploration of reaction pathways of converting CO_2 to other more useful chemicals.

$$CO_2 \rightarrow CO + O \tag{11.1}$$

$$CO \rightarrow C + O \tag{11.2}$$

$$C + CO \rightarrow C_2O \tag{11.3}$$

$$C_2O + CO \rightarrow C_3O_2 \tag{11.4}$$

$$C_3O_2 + O \rightarrow C_2O + CO_2 \tag{11.5}$$

$$C \rightarrow \text{graphite} \tag{11.6}$$

$$C_2O, C_3O_2 \rightarrow \text{polymers} \tag{11.7}$$

Wu et al. [6] studied reduction of CO_2 in aqueous solutions under γ-ray irradiation with the addition of many chemicals, including cuprous sulfite (Cu (II) and SO_3

$^{2-}$). Their original goal was to fixate CO_2 in the atmosphere. The authors investigated the effect of 22 compounds on the reduction of CO_2 dissolved in water. CO, CH_4, and C_2H_6 were measured after γ-ray exposure, and CO production yield on the order of 1% was the highest for a mixture of Na_2SO_3 and $CuSO_4$. On the other hand, Fe powder was most effective in terms of producing CH_4 and C_2H_6. The authors speculated that sulfite ions reacted with oxygen atoms to form sulfate ions as shown in Eqs. 11.8 and 11.9.

$$CO_2 + \gamma\text{-ray} \rightarrow CO + O \tag{11.8}$$

$$SO_3{}^{2-} + O \rightarrow SO_4{}^{2-} \tag{11.9}$$

No explanations were given as to how Cu(II) increased the yield of reaction 11.8. One possibility was that small Cu nanoparticles formed in solution catalyzed reaction 11.8 as speculated by Wu et al. in Tseng et al. [7] and Liu et al. [8].

Pilling et al. [9] studied the irradiation of ices of H_2O/CO_2 mixtures without any metal catalysts. They used 52 MeV Ni^{13+} ions and found that after an exposure to $2-3\times10^{12}$ ions/cm^2 irradiation, CO_2/CO and H_2O_2/H_2O were at fixed ratios of 0.1 and 0.01, respectively. Because of the high linear energy transfer (LET) associated with the ions, the yield of the products would be 1000 times lower if X-rays were used, putting CO_2/CO ratios around 100. Other products were also found, which included CO, O_3, CO_3, H_2CO_3, H_2O_2, formic acid, formaldehyde, and methanol.

These works are mentioned here because they studied mechanisms without nanomaterials. Other results of the study of decomposition of CO_2 and other molecules involving nanomaterials will be presented later in Sect. 11.3.

11.2.1.3 Radiolysis with Additives Including Nanomaterials

With the addition of nanomaterials, radiolysis can be enhanced. This is similar to catalysis described in Chap. 10, and the principles governing these processes are the same. The simplest explanation for the observed enhancement by nanomaterials is the increase of emission of elections that can directly decompose chemicals, either adsorbed on the surface of nanomaterials or in the surrounding. Notice that solvated electrons, although capable of reducing chemicals, cannot ionize or directly decompose chemicals. The increased production of energetic electrons can come from increased absorption of X-rays by nanomaterials, which belongs to types 1 and 2 physical enhancement described in Chap. 2. The enhancement can also come from the emission of UV-Vis light, which is type 3 physical enhancement described in Sect. 2.4.4.

The enhancement can also come from products catalyzed by nanomaterials under X-ray irradiation, which is chemical enhancement. If reactive oxygen species are increased through chemical processes such as catalysis, it is type 2 chemical enhancement. If there is no net increase of reactive oxygen species and there is still a measurable enhancement, then it is possible that type 1 chemical enhancement is in place. These pathways are discussed in Chap. 3.

11.2.2 Sensing

Research of nanomaterials to improve sensing of ionizing radiation has just begun. Both materials and methods are being explored. Transducers and readout devices are being developed as well. However, there are few reports to date, and the principles are largely underdeveloped. Here, the principles are only briefly speculated based on the existing literature. One example is to produce more stable radicals so that electron spin resonance (EPR) spectroscopy can be used to more directly determine the enhancement and the actual dose based on the amount of radicals produced. X-ray nanochemistry can be employed to enhance the effectiveness of X-ray irradiation and therefore the signal-to-noise ratio in the detection of ionizing radiation. However, currently the enhancement factor ranges from a fraction of one DEU to a few DEU. If the enhancement can be as large as two to three orders of magnitude higher when using systematically created nanomaterials and nanosystems, then it is possible to develop unique radiation sensors for personal usages and other purposes. In addition, new devices may be developed based on recent results of detection of radicals created in mixtures of nanoparticles and spin traps. Although these materials and devices have not yet developed into actual products that can be used in the field, it is foreseeable to develop them to meet special sensing needs in the future.

11.2.3 Environmental Remediation

X-ray nanochemistry can find applications in environmental work in several ways. The most straightforward way is to use X-ray nanochemistry to help decompose organic matter for environmental cleanup or remediation. Radiolysis enhanced by nanomaterials is the most straightforward way to accomplish this goal. The principles described in Sect. 11.2.1 are applicable here. However, currently there is still a large gap between what has been done and what can be done, and only a limited number of published reports are available in the literature. Nonetheless, many environmentally hazardous chemicals that are difficult to remove or destroy may be decomposed using methods developed in the future based on X-ray nanochemical principles. A list of these molecules is given here in Table 11.2.

Table 11.2 Environmentally unfriendly chemicals that can be decomposed using X-ray nanochemistry

Molecules	Toxicity
Perfluoroalkyl acid (PFAA)	Liver cancer
Perfluorooctanoic acid (PFOA)	Cancer
Polychlorinated dibenzo-p-dioxins (PCDD)	Cancer, disrupt hormone systems
Polychlorinated biphenyls (PCBs)	Cancer, attach immune systems
Dichlorodiphenyltrichloroethane (DDT)	May harm reproduction systems

11.3 Radiolysis with X-Rays and Nanomaterials as Catalysts

In Chap. 10 several aspects related to X-ray heterogeneous catalysis are covered. Here, the emphasis is placed on radiolytic decomposition of chemicals in the presence of nanomaterials under X-ray irradiation. In the past, much work was done with γ-rays, and these works are presented here because using X-rays in place of γ-rays can generally improve the efficiency of the γ-ray-driven chemical reactions if penetration depth is not restricted. When thick samples have to be used, then γ-rays should be more suitable. Reviews of this topic are available. For example, Meisel [10] reviewed radiolysis assisted with particles under ionizing radiation. Cecal and Humelnicu [11] reviewed the work in the area of hydrogen production in water with the assistance of nanomaterials under irradiation of ionizing radiation. These reviews provide helpful guidance to future work in this field.

11.3.1 Radiolysis of Water and Hydrogen Production Assisted by Nanomaterials

The most common experiment involving radiolysis is decomposition of water to produce hydrogen. This reaction has two merits. The first derives from production of hydrogen for fuels, and studying its production with ionizing radiation has a few advantages, including all-day operation of chemical production powered by background radiation or possible use of nuclear wastes. The second merit is the avoidance of the production of hydrogen, so that hydrogen production can be prevented in nuclear plants or waste containers to avoid dangerous situations such as explosion. The discussion here centers on these two themes.

One of the earliest studies using X-rays to produce hydrogen was done by Allen et al. [12]. The authors studied water hydrolysis under X-ray irradiation with additives other than nanomaterials. They employed hard X-rays emitted from bombarding a solid gold target with 2 MeV electrons. They measured hydrogen production from different solutions of ferrous sulfate and salt ($FeSO_4$, KBr, KI), peroxide, and oxygen. The authors considered that these ionic species must interact with hydrogen radicals to prevent the formation of hydrogen molecules. This pathway, if existed, would not forbid the use of catalysts.

Zeolite structures could also help radiolytic hydrogen gas formation. Masaki et al. [13] used two types of zeolites, NaY and HY, and found that HY was three times better than NaY. ^{60}Co was used as the radiation source and EPR spectroscopy was used to measure radicals. The measured G value was near 1.0, which was equivalent to 0.1 μmol J^{-1}. Apparently, these zeolites were not as effective as some of the oxides reported by Le Caer [14] (vide infra).

Okitsu et al. [15] employed both TiO_2 and Al_2O_3 particles and studied hydrogen production. The authors used γ-rays, and the results showed that Al_2O_3 enhanced the

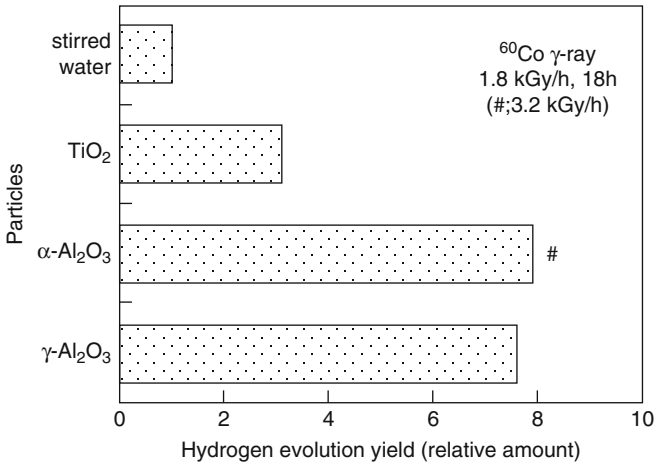

Fig. 11.1 Hydrogen production yield from four different samples, demonstrating the catalytic properties of oxide nanoparticles. (Reprinted from Okitsu et al. [15]. Copyright (1999) with permission from Elsevier.)

yield by 7–8 times. The surface morphology of Al_2O_3 and TiO_2 was different. The results are shown in Fig. 11.1. The authors also placed gold and other noble metals on the surface of these particles and found that Pt on TiO_2 was 2.2 times better than TiO_2. Metals on alumina apparently reduced the yield, and metals on TiO_2 were not as good as γ-Al_2O_3 alone.

Seino et al. [16] also found that adding TiO_2 or Al_2O_3 nanoparticles into water increased the yield of hydrogen production. They observed the dose dependency as well as the nanoparticle size dependency. 7–33 nm nanoparticles were used. The G values were low, on the order of 0.005–0.025. In another publication by Seino et al. [17], effect of pH on hydrogen generation by 30 nm titania nanoparticles was studied. The results suggested that there was little hydrogen production at a pH below 6 without nanoparticles. With nanoparticles, the yield of hydrogen gas production effectively occurred even at pH = 3.0.

In the early 2000s, Cecal et al. used several oxide nanosystems and different radiation sources to investigate hydrogen production. In a chapter in the book titled *Nuclear Power, Deployment, Operation and Sustainability*, Cecal et al. [11] discussed the production of hydrogen gas using several methods, including those methods that involved the assistance of zeolites and particles. The results are similar to the results discussed in Chap. 10.

LaVerne et al. [18] investigated radiolysis of water in the presence of CeO_2 and ZrO_2 microparticles. The authors used γ-rays and found a substantial increase in hydrogen production when the particles were added. They claimed that with one or two layers of water molecules on different particles, the yield of hydrogen production increased by a few fold over pure water. However, not all the particles performed the same way. They attributed the increase production of hydrogen to the increased production of excitons. They observed "drastic" difference between

these two particles. The authors revisited the same topic later [19]. In this latter work, they used dried particles and then treated the particles in different degrees of humidity and assumed that there were different layers of water on the surface of the particles prepared under these humidity settings. For one to two layers, the yield was very high, with the G value for H_2 production almost reaching 20 for CeO_2. For ZrO_2, the G value improved from 6 to 150. Energy transfer from the oxide to the water layer was discussed, although the transfer did not differ too much between CeO_2 and ZrO_2.

LaVerne et al. [20] observed that silica nanoparticles increased H_2 production when small silica nanoparticles (8–30 nm diameter) were used. Large silica particles in the slurry form did not generate any enhancement. The authors suggested that low-energy electrons emitted from small silica nanoparticles interacted with water and produced H_2. LaVerne [1] found that tetragonal nanoparticle ZrO_2 had greater activity than CeO_2 and was much better than the monoclinic ZrO_2 nanoparticles. The author suggested that annealing the nanoparticles from tetragonal to monoclinic resulted in loss of activity. G values were between 0.6 and 1.6. In comparison, water alone produced hydrogen at G value of 0.45 under γ-ray irradiation.

Renault et al. [21] studied radiolysis of water stored in pores of silica nanostructures. The yield was 0.3 in units of G value for hydrogen. The results did not change when hydroxyl radical scavengers were added. The authors claimed that nanowater was mainly responsible for the improved results of hydrogen production. The results are shown in Fig. 11.2.

Renault et al. [22] presented the results of their study of radiolysis of water in nanoporous gold. They prepared the gold samples by etching away Ag from a Ag-Au alloy. They reported a sevenfold increase in hydroxyl radical production

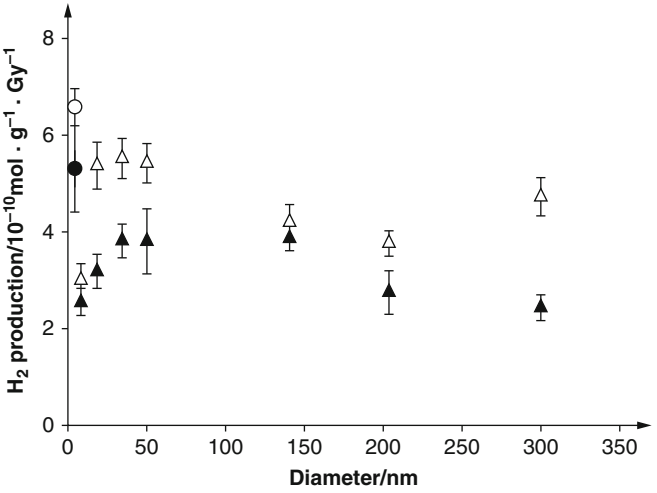

Fig. 11.2 Porous silica-assisted production of H_2. The pore size influenced the yield. Solid symbols are for dry glass samples, and empty symbols are for hydrated samples. A factor of two increase is visible for small pore silica. (Reprinted with permission from Renault et al. [21]. Copyright (2005) by John Wiley and Sons.)

near gold on short time scales. However, the production (or the increase) was suppressed by reactions with metal on long time scales. The results suggested that time-resolved measurements will be important. The authors used benzoic acid (BA) to react with hydroxyl radicals to form fluorescent products (similar to 3-CCA) to detect hydroxyl radicals. They considered the lifetime of the radical to be short, of the order of a few microseconds. The authors stated that BA was not as sensitive as coumarin but was used in a larger range of concentration. As the concentration of BA increased, the G value increased, suggesting that the lifetime was short or the distance between the gold surface and the radicals was small.

Maeda et al. [23] produced hydrogen by irradiating silica gel and metal oxide in water with ^{60}Co γ-rays. The silica gel apparently attracted water into their pores (1–2 nm size). The conditions of silica gel preparation, such as drying, were found to be important. Water absorbed on the surface of metal oxides was found to be easily hydrolyzed, which agreed with what Laverne et al. stated above. Two nm pore size was found to be optimal for maximum hydrogen production. This was slightly different from Gervais et al. [24] who found 10 nm pore size to produce the most solvated electrons. G values (H_2) were between 0.5 and 3. No enhanced absorption of γ-rays by nanomaterials was mentioned.

Meisel et al. [25] presented their results of using gold nanoparticles for hydrogen production in water. They studied size and surface effects of redox catalytic reactions. They stated that some reactions were affected by the presence of gold nanoparticles and some were not. In their discussion, they also clearly endorsed the idea of hydrogen radicals producing molecular hydrogen. The authors used 50 WP of gold, a significant amount, and attributed catalytic reduction of radicals to the observed results. The gold particles they used were microspheres of 1280 nm in diameter. The authors assumed the surface was important to the production of hydrogen. Figure 11.3 shows their results.

Meisel et al. [26] studied hydrogen production using silica-supported Ag nanoparticles. They used alcohol in the solution to scavenge radicals and obtained a G value of 0.45 for H_2 production. The H_2 G value increased from 1.1 without Ag to 1.9 with 0.12 mM Ag, although more Ag led to decrease of the G value.

The yield of organic reactions can also be increased by adding nanoparticles. Jung et al. [27] researched the effect of decomposition of ethylene diamine tetra acetic acid (EDTA) and found that addition of TiO_2 nanoparticles led to increased production of molecular hydrogen and destruction of EDTA molecules. This was possible because EDTA on TiO_2 stabilized reaction intermediates. The authors suggested that this method can be used to decompose harmful organic molecules while producing fuels such as hydrogen. Similar to nanomaterials, supramolecules may also help. A patent filed by Brewer et al. [28] described how to use supramolecules of Ru and Rh compounds under visible light to produce hydrogen. These molecules were known as photocatalysts. It is possible that these molecules can also produce hydrogen under X-rays or other ionizing radiation.

Yoshida et al. [29] used 3 μm or larger $A_{12}O_3$ particles to study hydrogen production under γ-ray irradiation and found that compared to water alone, adding these particles led to the increase in the yield of hydrogen production by two orders

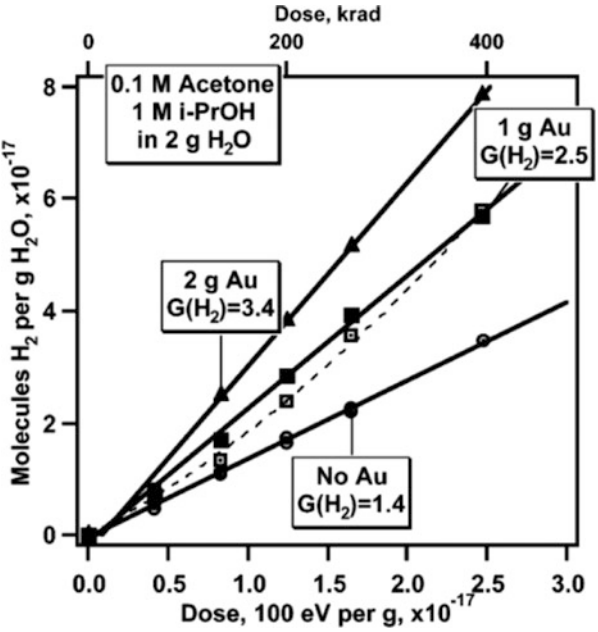

Fig. 11.3 Gold nanoparticle-assisted production of H_2. Enhancement is visible when gold was added, and the enhancement was approximately 1.0 DEU per 100 WP of gold in water, suggesting that the gold was highly scavenging even though it provided physical enhancement. (Adapted with permission from Meisel et al. [25]. Copyright (2006) American Chemical Society.)

of magnitude. The largest particles they used were 6 mm in diameter. ^{60}Co at a dose rate of 4.57 kGy/h was used for irradiation. Hydrogen produced was between 0.3 and 3.48 μmol/mL, which were much higher than the 0.0134 μmol/mL obtained from pure water. The enhancement could come from several factors including physical enhancement discussed in Chap. 2 and possibly chemical enhancement discussed in Chap. 3.

In a similar study, Kumagai et al. [30] investigated radiolysis of mordenite in sea water under γ-ray irradiation. Hydrogen production was monitored. The authors attributed the additional production of hydrogen to the energy absorbed by mordenite at the yield of 2.3×10^{-8} mol/J. Addition of seawater increased hydrogen production, which was attributed to the salt present in seawater.

Gervais et al. [24] theoretically examined the production of electrons and hydroxyl radicals by irradiation of silica nanoparticles in water with 50 keV electrons. The authors studied the role of the energy levels or band structure of water and silica and recognized that the bandgap of silica was slightly greater than that of water. The results showed that the production of electrons and hydroxyl radicals was heavily influenced by the pore size of silica, with electron production more sensitively dependent on the pore size. Although as stated in Chap. 2 that the difference between cross-sections of ionization of gold and water for electrons is much smaller

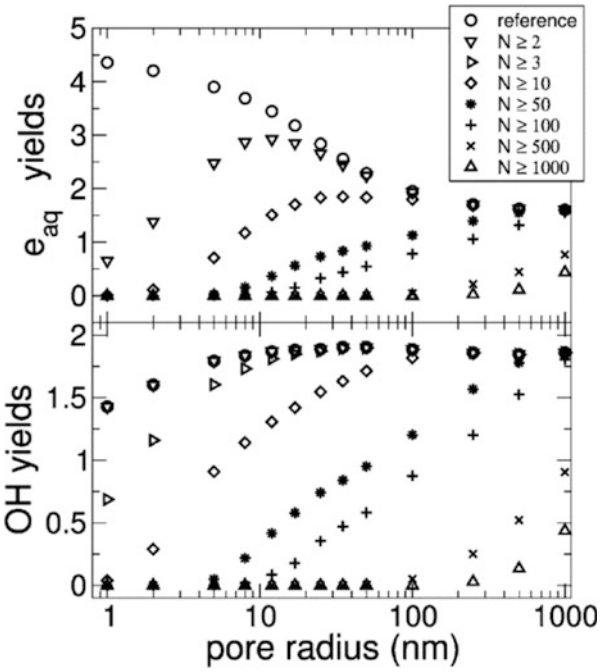

Fig. 11.4 Yield of solvated electron and hydroxyl radical production as a function of the pore size of porous silica under irradiation. (Adapted with permission from Gervais et al. [24]. Copyright (2010) American Chemical Society.)

than X-rays, electron attachment and vibrational excitation of water were more efficient than X-rays for water and silica. The results showed that species such as solvated electrons and hydroxyl radicals in each pore changed as a function of pore size, as shown in Fig. 11.4. Particularly, the results showed the production of solvated electrons was optimal for 10 nm pore size silica.

Mostafavi et al. [31] studied the effect of TiO_2 nanoparticles on hydrogen production by ^{60}Co γ-ray irradiation as well as by 28 MeV $^4He_2^+$ ions. Mass spectrometry was used to measure hydrogen production, and G values were between 0.135 and 0.19 for ion irradiation. Ion irradiation caused the G value (H_2) to increase from 1.04 to 1.35. For γ-rays, the G value increased to 0.53, which was higher than the ions.

Le Caer [14] reviewed water radiolysis and discussed the influence of oxide surfaces on hydrogen production under ionizing radiation. The time frame in which radiolysis occurred was described. The yields of radiolytic reaction products for different irradiation particles were given. The results are listed in Table 11.3. The conclusion of the review indicated that hydrogen production strongly depends on the surface of oxides. The author also mentioned that very efficient energy transfer could take place at the interface.

Solvated electrons were studied by Crowell et al. [32]. They used 1–57 nm pore size silica to study solvated electrons using absorption spectroscopy. The authors considered the water in the pores as nanowater and found such water behaves differently from regular water, similar to the findings made by Renault et al. and

Table 11.3 Radiolytic yields (μmol J^{-1}) for γ-rays and high-energy electrons as given by Le Caer in [14]. γ-rays and electrons both have a linear energy transfer (LET) rate of 0.2–0.3 keV μm^{-1}

Radiation	e_{aq}^-	•OH	•H	H_2	H_2O_2	$•O_2H$
γ and electrons (0.1–10 MeV) (pH = 3–11)	0.28	0.28	0.06	0.047	0.073	0.0027

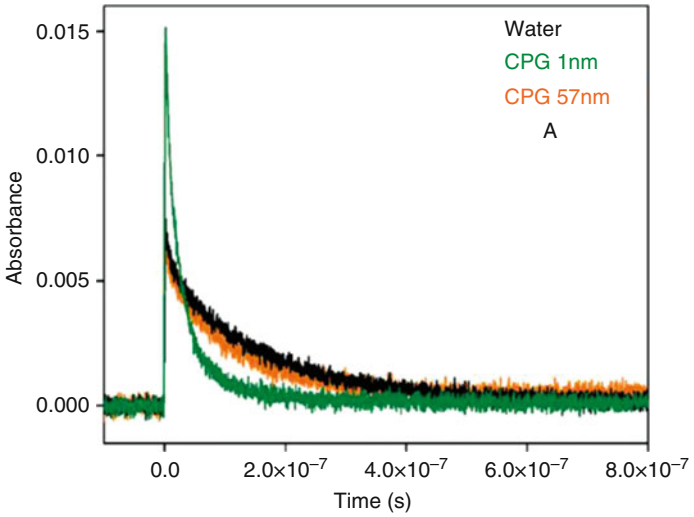

Fig. 11.5 Nanowater in porous silica for assisted production of H_2. Solvated electron signals are shown here. There is a sharp difference between small pores (1 nm) and the bulk water or water in large pores (57 nm). (Adapted with permission from Crowell et al. [32]. Copyright (2012) American Chemical Society.)

Laverne et al. mentioned earlier. It was found that initial yields of solvated electrons doubled as the pore size decreased from 57 nm (whose results are close to bulk water) to 1 nm. Clearly, silica of different pores behaved differently. Since the pore size was not continuously adjusted, the result shown in Fig. 11.5 could not be directly compared with Gervais et al. [24].

Frances et al. [33] investigated hydrogen production following radiolytic reactions under γ-ray irradiation of water in zeolites. ^{137}Cs was used for irradiation, and zeolite 4A was used for the experiment. The results of hydrogen production are shown in Fig. 11.6. Adding zeolites increased hydrogen production by nearly threefold. Their work was the basis of a more recent study done by Frances et al. [34], who studied self-radiolysis of tritiated water stored in zeolite 4A. The zeolite was noted to play two roles. First, it increased decomposition of water by providing energy to the trapped water. Secondly, it enhanced recombination of major stable radiolytic products. These explanations could also apply to the γ irradiation study whose results are shown in Fig. 11.6.

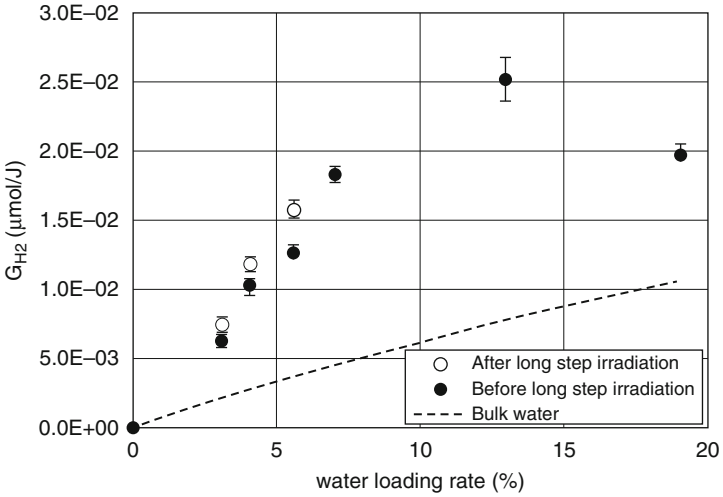

Fig. 11.6 Zeolite-assisted production of H_2. Under γ-ray irradiation. Optimal loading of water was 13%. (Reprinted from Frances et al. [33]. Copyright (2015) with permission from Elsevier.)

These experiments can be further optimized for future nanomaterials under X-ray irradiation. The photocatalysts for hydrogen production to date have not been optimized, and the overall yield (quantum efficiency) is still low, below 5% in most cases. X-ray photolysis of water may benefit from general photolysis work and provides useful supporting information for unique catalytic systems for photolysis of water.

11.3.2 Radiolysis of CO_2 with X-Rays Assisted by Nanomaterials

Works discussed in this subsection are part of X-ray nanochemistry. Although some of them may not employ catalysts, nanomaterials are involved. In one example, Fujita et al. [35] reported the results of pH-dependency measurements of γ-ray (from ^{60}Co) irradiated iron-containing water solutions saturated with CO_2. Fe powder with 29 m^2/g unit mass surface area was used in the work. The authors found that pH decreased quickly after irradiation. The authors stated that H^+ generation was significantly increased by adding CO_2 to water. pH decreased to about 2.2 after a few minutes of 100–200 Gy irradiation, and pH gradually recovered to 3.5 after irradiation. Adding Ar instead of CO_2 increased the final pH from 3.5 to 4.5. Initial H^+ change was the highest when ~0.1 g Fe powder was added. Several factors were considered to contribute to the increased production of protons.

Another example was shown by Yoshida et al. [36] who investigated decomposition of CO_2 by metals under γ-ray irradiation. They used metals to increase the

Table 11.4 Theoretical and experimental yields of CO production from γ-ray irradiated metals according to Yoshida et al. [36]

Materials	Surface area (cm^2)	Yield ($\times 10^{-3}$)	Electron yield (theoretical)
Pure water		0.21	0.13
Stainless steel	2780	0.73	0.18
Stainless steel	30,100	1.43	0.18
Lead	2780	1.30	0.33

absorption of γ-rays to emit low-energy electrons. CO yield was measured. The authors also theoretically studied electron emission from different metals under ^{60}Co 1.3 MeV γ-ray irradiation. Since γ-ray absorption cross-sections for different elements are similar, which are within a factor of two among the metals studied, the increase was mainly caused by the difference in density between the nanomaterials and water. This was different from gold in water under X-ray irradiation in which the absorption cross-section of gold was two orders of magnitude higher than oxygen. The experimental results showed that CO production quadrupled as the metal volume increased for the metals used in the experiments. The measured yield of decomposition was the highest for stainless steel mesh, possibly due to the tenfold higher surface area compared to lead plates, even though the latter had a higher Z value as well as higher density. When similar stainless steel plates were used, lead plates produced twice as much CO, which agreed with the theoretical results. Table 11.4 lists the relevant results. The volume of the metals was held constant.

11.3.3 Decomposition of Hydrogen Peroxide

H_2O_2 is another molecule that can be decomposed with ionizing radiation. Only the results obtained with nanomaterials and were not spontaneously catalyzed are discussed here because many metal nanoparticles spontaneously catalyze the decomposition of H_2O_2. For example, gold or silver surfaces could decompose H_2O_2 even without X-ray irradiation. Dependency on pH and other variables were explored by several groups as well. These works established that gold and silver surfaces were intrinsically catalytically active toward the decomposition of H_2O_2. It was therefore interesting to investigate how ionizing radiation worked with nanomaterials that normally would not catalyze the decomposition of H_2O_2. It is worth noting that ionizing radiation itself can also produce a small amount of H_2O_2 in water, which further complicates the decomposition process.

LaVerne et al. [37] discussed the decomposition of H_2O_2 at high temperatures assisted with ceramic oxides under irradiation of ^{60}Co γ-rays. The sizes of the ceramic particles were large, on the order of 117–641 nm. The results indicated that some oxides, such as CeO_2 and ZrO_2, dramatically increased H_2O_2 decomposition. Figure 11.7 shows the results. The Arrhenius constants for CeO_2 and ZO_2 were 1.7×10^3 and 3.8×10^4 $s^{-1}m^{-2}$, which were one to two orders of magnitude

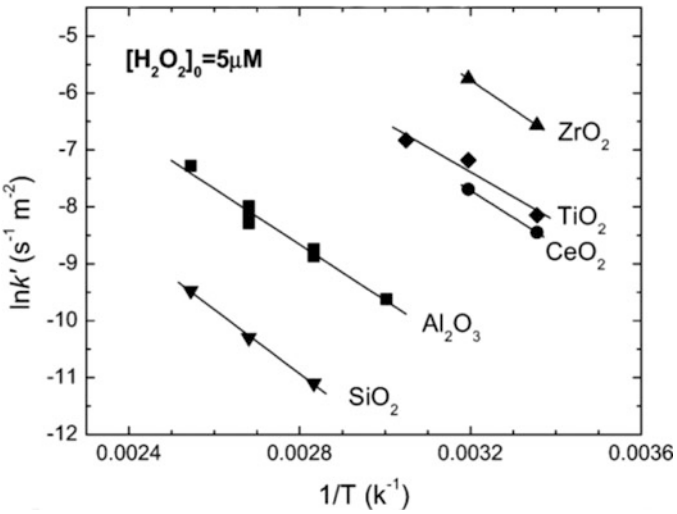

Fig. 11.7 Hydrogen peroxide decomposition in the presence of ceramic oxides under γ-rays. (Adapted with permission from LaVerne et al. [37]. Copyright (2005) American Chemical Society.)

higher than those for SiO_2 or Al_2O_3. The activation energies, on the other hand, were 5 kJ mol^{-1} and 41 kJ mol^{-1}. Catalysis can be studied without ionizing radiation for comparison purposes because Pt nanoparticles are also catalytically active in the presence of H_2O_2. Nonetheless, when irradiated with ionizing radiation, the mechanisms are different due to participation by other active species.

Guo et al. [38] studied a new nanomaterial they called Agu that had less than a 2 nm layer of silver coated on approximately 100 nm gold nanospheres. The surface plasmon resonance (SPR) response of this material (see Chap. 6 for details) followed a sigmoidal function with respect to silver thickness, with the most sensitive region (measured by growth) being between 0.9 and 1.6 nm of silver thickness. Either H_2O_2 or X-rays could remove the silver layer, creating the sensitive sigmoidal response. In the process, H_2O_2 was decomposed, although it followed a complex pathway.

11.3.4 Decomposition of Large Molecules

Yoshida et al. [39] discovered that adding metals increased the degradation of chemicals in solutions such as dibutyl phthalate (DBP) in water. They used γ-rays and observed an increase in the yield of degradation in the presence of metal (Al, Ni, Mo, W, and Pb) plates. The energy of γ-rays was 1.3 MeV, and the dose was 50 Gy; the DBP peak was almost gone after 44 kGy of irradiation, determined by UV absorption spectroscopy. The authors also theoretically studied energy dependency and found that 200–400 keV were optimal. W and Mo metals were found to be the most efficient elements for degradation. Pb was only 25% as effective.

The largest molecules decomposed by ionizing radiation, such as X-rays, with the assistance of nanomaterials were plasmid DNA strands of a few thousand base pairs. Several works were reported in the literature, and increased yields were reported in the presence of gold nanoparticles of different sizes. For example, Guo et al. [40], Guo et al. [41] and [42], and McMahon et al. [43] all reported enhanced damage to plasmid DNA molecules, and their results are shown in Chap. 3 in the form of chemical enhancement. It is important to point out that regardless of the true enhancement mechanisms, the degree of damage to these large molecules was increased significantly with the addition of gold nanoparticles. The increases were much higher than those predicted based on physical enhancement.

11.4 Sensing Applications Using X-Ray Nanochemistry

Miller et al. [44] from IBM reported on using polysilanes as radiation sensitizing materials. The original work did not include nanomaterials or X-rays. The results showed chain scission and molecular reduction upon irradiation with 248 nm light. The authors speculated the involvement of silyl radicals. It was possible that X-rays or other types of ionizing radiation could produce similar results.

Mulvaney et al. [45] discussed a new nanomaterial with which the authors used to detect electrons trapped in gold nanoparticle cores coated with a layer of porous SnO_2. The gold nanoparticles were 15 nm in diameter and were covered with a 10 nm thick layer of SnO_2. Upon irradiation with γ-rays, the authors stated that approximately 2000 electrons or negative charges were trapped in each gold nanoparticle core.

Quantum dots may be used as radiation sensors. Gao et al. [46] examined the possibility of using ZnO and CdTe quantum dots to detect superficial X-rays from 36.9 to 64.9 keV, at which energy physica enhancement from gold nanoparticles in water is the highest. The size of these two quantum dots was between 1 and 8 nm based on SEM measurements. Their results showed more uniform response in this energy range for CdTe than ZnO quantum dots. The authors compared the performance of the quantum dot sensors with other contemporary sensors.

A number of chemicals were used together with EPR spectroscopy to enhance the effectiveness of X-ray irradiation and function as sensors. Formates and dithionates were good candidates, as demonstrated by Lund et al. [47]. Guidelli et al. [48] discussed the use of silver nanoparticles to increase the sensitivity of alanine for EPR detection of carbon radicals derived from alanine. The results are shown in Fig. 11.8. These were promising results for medical applications but far below the requirements for making sensors to detect background radiation. In principle, it is possible to use X-ray nanochemistry to further improve the sensitivity of these existing sensors of ionizing radiation.

Marques et al. [49] reported a dosimetric study of MAGIC-f gel mixed with gold nanoparticles. They irradiated the samples with 250 kVp X-rays and a 5 Gy exposure. With 0.02–0.1 mM gold concentrations, the authors observed an up to 106%

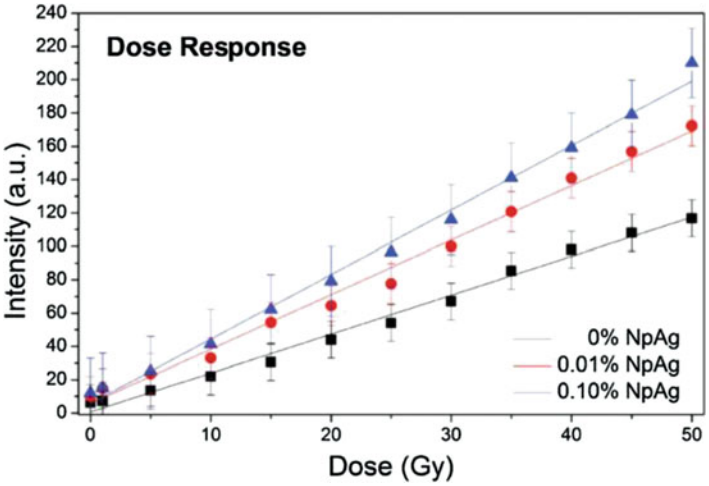

Fig. 11.8 EPR measurement of silver nanoparticle enhanced radical production. Responses to dose are shown for three silver concentrations. (Adapted with permission from Guidelli et al. [48]. Copyright (2012) American Chemical Society.)

increase in response or a 1.06 DEU enhancement, which began to plateau above 0.02 mM. The enhancement was determined by the nuclear magnetic transversal relaxation rate (R2). The results are shown in Fig. 11.9. The measured enhancement values were compared with the theoretically predicted values, and the authors claimed that there was a close matching between the two sets of data. The approach demonstrated the potential of using nanomaterials to advance methods of radiation sensing.

Alqathami and Geso et al. [50] explored dose enhancement in gold nanoparticle-embedded tissue-equivalent mixtures irradiated with 100 kV and 6 MV X-rays. The authors mixed polyurethane resin precursors with initiators and LMG dye molecules to make the tissue-equivalent material. Gold nanoparticles were mixed with these chemicals to enhance absorption of X-rays. The average size of the gold nanoparticles was 50 nm. The enhancement was determined based on the ratio of slopes of optical density change as a function of X-ray dosage with gold nanoparticles to without gold nanoparticles. The loading of gold was only 0.5 mM or 0.01 WP (0.098 g/1000 g). The enhancement for 100 kVp and 6 MV was 1.77 and 1.1 DEU, respectively. Figure 11.10 shows their results, which show an enhancement of approximately 1.0 DEU.

Rakowski et al. [51] developed a composite material consisting of a nanofilm of gold deposited on top of a radiochromic film to detect the enhancement from the gold film, which was 23 nm thick. Under irradiation of 50 kVp X-rays, the dose enhancement ratio (DER) was 0.29 DEU integrated within 13.6 μm of water. The authors also theoretically simulated the enhancement and found that maximum DER reached 18 DEU within 250 nm of the gold film.

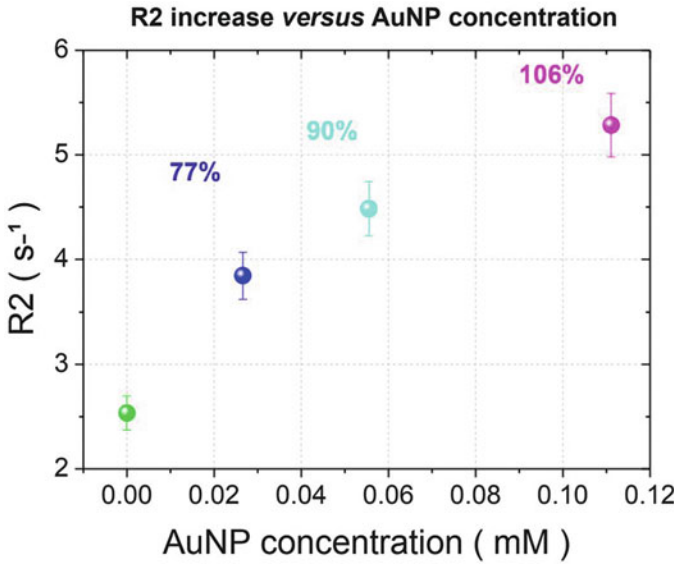

Fig. 11.9 R2 measurement of enhancement using gold nanoparticles. (Adapted from Marques et al. [49]. Used with permission, CC BY 2.0. © Institute of Physics and Engineering in Medicine. Reproduced by permission of IOP Publishing. All rights reserved.)

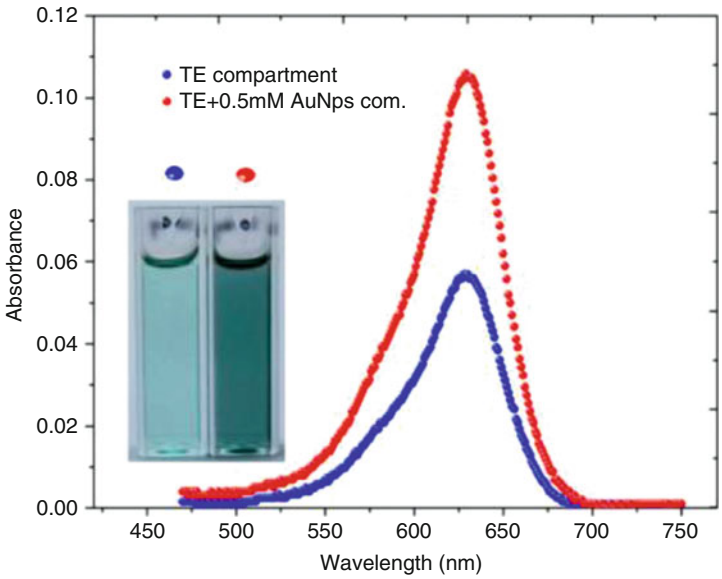

Fig. 11.10 Enhancement of dosimeter performance by gold nanoparticles. LMG dye immersed in polyurethane resin was used as the matrix to respond to X-ray irradiation. Color change was detected with UV-Vis spectroscopy. (Reprinted from Alqathami and Geso et al. [50]. Copyright (2013) with permission from Elsevier.)

Rege et al. [52] reported a method of using ionizing radiation to produce gold nanoparticles from specially prepared gold ions in the sensing solution. Colorimetry was used to determine the dosage. The lowest dose detected was 0.5 Gy of ionizing radiation. The key was to prepare ions before irradiation so that they were easily reduced by a small amount of reducing agents produced by ionizing radiation. In this work, Au(III) was reduced to Au(I) chemically prior to radiation, similar to aged Au ions used in the synthesis of gold nanotubes employed by Guo et al. [42]. In addition to aging, cetyl trimethylammonium bromide (CTAB) ligands were used to increase the probability of aggregation of gold atoms to form small gold nanoparticles. Rege et al. [53] developed a new dosimetric tool that uses colorimetric plasmonic response from gold nanoparticles formed in situ under X-ray irradiation. Gold salt was poured into a gel that also had cetyl or dodecyl trimethylammonium bromide (C_xTAB, $x = 16$ or 12) and ascorbic acid. Under X-ray irradiation, the gel changed color as gold ions were reduced to form nanorods or nanoparticles. They called the nanoparticle forming solution under X-ray irradiation a nanosensor. As little as 0.5 Gy of X-ray, irradiation was detected. Such a method allowed convenient determination of the X-ray dose used in tumor treatment.

The Agu work performed recently by Guo et al. [38] could also aid sensing. A thin silver coating on spherical gold nanospheres could be used as an indicator to detect X-rays or other chemical etching reagents. A segment of a sigmoid response observed as a function of thickness of silver is shown in Fig. 11.11. The thickness change to the silver layer could be caused by either chemical etching or irradiation of X-rays. This new nanomaterial exhibited a sensitive surface plasmon resonance (SPR) response when the thickness of silver was changed from 0.9 to 1.6 nm on approximately 100 nm diameter gold nanospheres. To remove the surface silver, the authors employed X-ray radiation from a 100 kVp microfocus source and irradiated aqueous solutions. Figure 11.11 also shows the results of SPR peak shifts as a function of X-ray dose. Although a large dose of X-rays (i.e., ~100 Gy) was needed to cause significant SPR peak shift, it was possible to detect <40 Gy of X-ray irradiation based on the SPR shift.

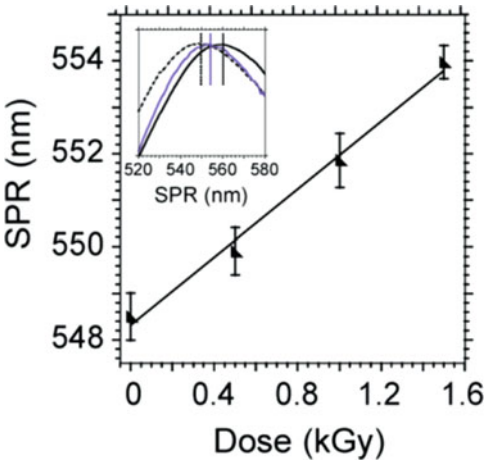

Fig. 11.11 Etching of silver from Agu under X-ray irradiation detected by surface plasmon resonance (SPR) absorption spectroscopy. SPR shift was 2 nm per 400 Gy of X-ray irradiation. The centroid of SPR profiles could be determined with a 0.25 nm resolution. (Reprinted from Guo et al. [38]. Copyright (2016) with permission from Elsevier.)

Another recent work related to sensing was the study of a new concept of X-ray-induced energy transfer (XIET) reported by Guo et al. [2] in which relative energy transfer efficiencies in the form of dose enhancement were measured. The experimental illustration is given in Sect. 2.4.3.4. In this study, the authors demonstrated that energy transfer from nanomaterial donors made of heavy elements to the nearby nanomaterial acceptors made of light elements could be used to sense ionizing radiation. The chemical content in the acceptors was modified by the energy transfer upon irradiation, and the degree of modification can be quantified with enhancement defined in Chaps. 2, 3, 4, and 5. For example, the enhancement could be measured by sending nanoparticle probes in the acceptors into a sensing region buried deep in an optically opaque object that is relatively transparent to X-rays. The opaque object with the acceptors is then irradiated with X-rays, and the probes are retrieved and measured. The enhancement or XIET efficiency is higher for those nanoscale probes positioned within nanometers of the target of materials made of heavy elements.

11.5 Environmental Research Applications Using X-Ray Nanochemistry

Mitomo et al. [54] studied degradation of poly(L-lactic acid) under irradiation of γ-rays. As the damage was believed to be caused by radicals, using X-rays should give rise to better results than γ-rays. However, the dose they used was up to 200 kGy, which was on the high end of the dose employed in the research described in this book. This dose may be reduced when X-rays are used, due to stronger interactions between the molecules and X-rays. The work also did not use nanoparticles. If nanoparticles were used, then the amount of damage should be increased, which can further reduce the dose. The results showed that as the dose increased, the melting temperature and average molecular weight decreased. There seemed to be saturation beyond initial 200 kGy of irradiation based on the average molecular data (right panel in Fig. 11.12). On the other hand, the melting temperature results (left panel in Fig. 11.12) did not follow the same trend. The authors attributed the saturation observed in the average molecular weight results to the recombination reaction of free radicals.

Hoertz et al. [55] investigated radiocatalytic degradation of organic species with the assistance of nanomaterials. They employed γ-rays and semiconductor nanoparticles Al_2O_3, TiO_2, and ZrO_2. The work focused on several types of TiO_2 nanomaterials, including annealed and unannealed homemade nanopowder, as well as commercially available nanoparticles. The authors found that the most promising material was TiO_2 under ^{60}Co irradiation to decompose sulforhodamine molecules. The targets were mixed with nanomaterials in aqueous solutions. They attributed the damage to hydroxyl radicals produced in the solution based on the existing literature on the subject.

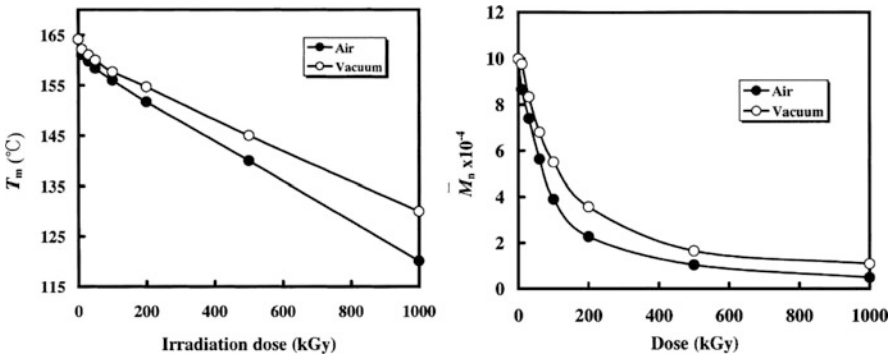

Fig. 11.12 Degradation of poly(L-lactic acid) under irradiation. Melting temperature and average molecular weight were measured and shown in the left and right panel, respectively. No nanoparticles were used. (Reprinted from Mitomo et al. [54]. Copyright (2001) with permission from Elsevier.)

11.5.1 Nanomaterials under X-Ray Irradiation for Remediation

Adding nanomaterials should increase decomposition of chemicals in the environment by X-rays. As shown in Chaps. 2, 3, 4, and 5, nanomaterials help increase the effectiveness of X-ray irradiation. As long as the nanomaterials are not toxic to the environment, they can be used as environmental remediation reagents. Although X-rays have not been used as the energy source to treat contaminated water or soil, it is foreseeable that inexpensive nanomaterial catalysts in combination with X-rays may be developed in the future to selectively treat the toughest contamination in the environment.

11.5.2 Nanomaterials as Protection Reagents

As shown in Chap. 3, not all nanomaterials can enhance the effectiveness of X-ray irradiation. Most nanomaterials actually do the opposite, which is to reduce the effectiveness of X-ray irradiation unless special care is taken with respect to the preparation of the nanomaterials. In these cases, nanomaterials can protect certain parts of the environment. To date, only a few systematic works have been done in the area of creating the best X-ray or ionizing radiation antidotes. Ironically, iodide is one of the recommended ionizing radiation antidotes but was also one of the best candidates for Auger therapy before the discovery of nanomaterials as radiation sensitizers. Many ionizing radiation antidotes are chemical compounds and may be conjugated to nanomaterials to improve their effectiveness. Liu et al. [56] reported

conjugation of Trolox, a vitamin E analogue and a reactive oxygen scavenger, to gold nanoparticles. The product, AuNP@Trolox, was found nine times more scavenging than Trolox.

11.6 Conclusions and Future Work

Radiolysis, sensing, and environmental remediation work are the three areas of application of X-ray nanochemistry described in this chapter. Basic principles are briefly reviewed. Publications in these three areas are reviewed, and though they are encouraging, not all of them involve both nanomaterials and X-rays. Many of the works reviewed here use γ-rays, whose results should be predictably improved if X-rays are instead utilized. For those publications using bulk metals, the results should also see improvements when nanomaterials are used.

The existing literature in these three areas only reveals a glimpse of what X-ray nanochemistry may accomplish. There are many possibilities of using X-ray nanochemistry to improve radiolysis, sensing, and environmental work. Future sensing devices may be developed using new principles similar to those shown in Chaps. 2, 3, 4, and 5. As X-rays are convenient to use and highly penetrating, X-ray nanochemistry may have more profound impacts in all three areas.

It is also possible that these applications will provide valuable feedback on how to improve X-ray nanochemistry. For example, sensing may be used to report enhancement; if X-ray to signal conversion efficiency is high enough or can be amplified, then sensing may become a sensitive method to determine enhancement. Similarly, radiolytic methods can help improve the enhancement or enhancement measurements. Future work will bridge these gaps between applications and fundamental aspects of X-ray nanochemistry.

References

1. LaVerne, J. A. (2005). H_2 formation from the radiolysis of liquid water with zirconia. *The Journal of Physical Chemistry. B, 109*, 5395–5397.
2. Sharmah, A., Yao, Z., Lu, L., & Guo, T. (2016). X-ray-induced energy transfer between nanomaterials under X-ray irradiation. *Journal of Physical Chemistry C, 120*, 3054–3060.
3. Farhataziz, & Rodgers, M. A. J. (1987). *Radiation chemistry: Principles and applications* (p. 527). New York: VCH Publishers, Inc..
4. Harteck, P., & Dondes, S. (1955). Decomposition of carbon dioxide by ionizing radiation. 1. *The Journal of Chemical Physics, 23*, 902–908.
5. Kummler, R., Leffert, C., Im, K., Piccirelli, R., Kevan, L., & Willis, C. (1977). Numerical-model of carbon-dioxide radiolysis. *The Journal of Physical Chemistry, 81*, 2451–2463.
6. Wu, X. Z., Hatashita, M., Enokido, Y., & Kakihana, H. (2000). Reduction of carbon dioxide in gamma ray irradiated carbon dioxide: Water system containing Cu^{2+} and SO_3^{2}. *Chemistry Letters, 29*, 572–573.

7. Tseng, I. H., Chang, W. C., & Wu, J. C. S. (2002). Photoreduction of CO_2 using sol-gel derived titania and titania-supported copper catalysts. *Applied Catalysis B: Environmental, 37*, 37–48.
8. Liu, D., Fernandez, Y., Ola, O., Mackintosh, S., Maroto-Valer, M., Parlett, C. M. A., Lee, A. F., & Wu, J. C. S. (2012). On the impact of Cu dispersion on CO_2 photoreduction over Cu/TiO_2. *Catalysis Communications, 25*, 78–82.
9. Pilling, S., Duarte, E. S., Domaracka, A., Rothard, H., Boduch, P., & da Silveira, E. F. (2010). Radiolysis of H2O:CO2 ices by heavy energetic cosmic ray analogs. *Astronomy and Astrophysics, 523*, *A77*.
10. Meisel, D. (2004). Radiation effects in nanoparticle suspensions. In L. M. Liz-Marzán & P. V. Kamat (Eds.), *Nanoscale materials* (pp. 119–134). New York: Kluwer Academic Publishers.
11. Cecal, A., & Humelnicu, D. (2011). Hydrogen output from catalyzed radiolysis of water. In P. Tsvetkov (Ed.), *Nuclear power – Development, operation and sustainability* (pp. 489–510). Rijeka: InTech.
12. Johnson, E. R., & Allen, A. O. (1952). The molecular yield in the decomposition of water by hard X-rays. *Journal of the American Chemical Society, 74*, 4147–4150.
13. Nakashima, M., & Masaki, N. M. (1996). Radiolytic hydrogen gas formation from water adsorbed on type Y zeolites. *Radiation Physics and Chemistry, 47*, 241–245.
14. Le Caer, S. (2011). Water radiolysis: Influence of oxide surfaces on H_2 production under ionizing radiation. *Water, 3*, 235–253.
15. Yamamoto, T. A., Seino, S., Katsura, M., Okitsu, K., Oshima, R., & Nagata, Y. (1999). Hydrogen gas evolution from alumina nanoparticles dispersed in water irradiated with gamma-ray. *Nanostructured Materials, 12*, 1045–1048.
16. Seino, S., Yamamoto, T. A., Fujimoto, R., Hashimoto, K., Katsura, M., Okuda, S., & Okitsu, K. (2001). Enhancement of hydrogen evolution yield from water dispersing nanoparticles irradiated with gamma-ray. *Journal of Nuclear Science and Technology, 38*, 633–636.
17. Seino, S., Yamamoto, T. A., Fujimoto, R., Hashimoto, K., Katsura, M., Okuda, S., & Okitsu, K. (2001). Effect of pH on hydrogen evolution yield from water dispersing tirania nanoparticles enhanced by gamma ray. *Materials Research Society Symposia Proceedings, 676*, Y3.43.41–45.Y3.43.1.
18. LaVerne, J. A., & Tandon, L. (2002). H_2 production in the radiolysis of water on CeO_2 and ZrO_2. *The Journal of Physical Chemistry. B, 106*, 380–386.
19. Roth, O., Dahlgren, B., & LaVerne, J. A. (2012). Radiolysis of water on ZrO2 nanoparticles. *Journal of Physical Chemistry C, 116*, 17619–17624.
20. LaVerne, J. A., & Tonnies, S. E. (2003). H_2 production in the radiolysis of aqueous SiO_2 suspensions and slurries. *The Journal of Physical Chemistry. B, 107*, 7277–7280.
21. Rotureau, P., Renault, J. P., Lebeau, B., Patarin, J., & Mialocq, J. C. (2005). Radiolysis of confined water: Molecular hydrogen formation. *ChemPhysChem, 6*, 1316–1323.
22. Musat, R., Moreau, S., Poidevin, F., Mathon, M. H., Pommeret, S., & Renault, J. P. (2010). Radiolysis of water in nanoporous gold. *Physical Chemistry Chemical Physics, 12*, 12868–12874.
23. Maeda, Y., Kawana, Y., Kawamura, K., Hayami, S., Sugihara, S., & Okaib, T. (2005). Hydrogen gas evolution from water included in a silica gel cavity and on metal oxides with γ-ray irradiation. *Journal of Nuclear and Radiochemical Sciences, 6*, 131–134 131.
24. Ouerdane, H., Gervais, B., Zhou, H., Beuve, M., & Renault, J. P. (2010). Radiolysis of water confined in porous silica: A simulation study of the physicochemical yields. *Journal of Physical Chemistry C, 114*, 12667–12674.
25. Merga, G., Milosavljevic, B. H., & Meisel, D. (2006). Radiolytic hydrogen yields in aqueous suspensions of gold particles. *The Journal of Physical Chemistry. B, 110*, 5403–5408.
26. Zidki, T., Cohen, H., Meyerstein, D., & Meisel, D. (2007). Effect of silica-supported silver nanoparticles on the dihydrogen yields from irradiated aqueous solutions. *Journal of Physical Chemistry C, 111*, 10461–10466.
27. Jung, J., Jeong, H. S., Chung, H. H., Lee, M. J., Jin, J. H., & Park, K. B. (2003). Radiocatalytic H_2 production with gamma-irradiation and TiO_2 catalysts. *Journal of Radioanalytical and Nuclear Chemistry, 258*, 543–546.

28. Brewer, K. J., & Elvington, M.. (2006). Supramolecular complexes as photocatylysts for the production of hydrogen from water. US 7122171 B2.
29. Yoshida, T., Tanabe, T., Sugie, N., & Chen, A. (2007). Utilization of gamma-ray irradiation for hydrogen production from water. *Journal of Radioanalytical and Nuclear Chemistry, 272*, 471–476.
30. Kumagai, Y., Kimura, A., Taguchi, M., Nagaishi, R., Yamagishi, I., & Kimura, T. (2013). Hydrogen production in gamma radiolysis of the mixture of mordenite and seawater. *Journal of Nuclear Science and Technology, 50*, 130–138.
31. Essehli, R., Crumiere, F., Blain, G., Vandenborre, J., Pottier, F., Grambow, B., Fattahi, M., & Mostafavi, M. (2011). H-2 production by gamma and He ions water radiolysis, effect of presence TiO2 nanoparticles. *International Journal of Hydrogen Energy, 36*, 14342–14348.
32. Musat, R. M., Cook, A. R., Renault, J. P., & Crowell, R. A. (2012). Nanosecond pulse radiolysis of Nanoconfined water. *Journal of Physical Chemistry C, 116*, 13104–13110.
33. Frances, L., Grivet, M., Renault, J. P., Groetz, J. E., & Ducret, D. (2015). Hydrogen radiolytic release from zeolite 4A/water systems under gamma irradiations. *Radiation Physics and Chemistry, 110*, 6–11.
34. Frances, L., Douilly, M., Grivet, M., Ducret, D., & Theobald, M. (2015). Self-radiolysis of tritiated water stored in zeolites 4A: Production and behavior of H_2 and O_2. *Journal of Physical Chemistry C, 119*, 28462–28469.
35. Fujita, N., Fukuda, Y., Matsuura, C., & Saigo, K. (1996). Radiation-enhanced H^+ generation in iron-containing solution saturated with CO_2. *Radiation Physics and Chemistry, 48*, 297–304.
36. Yoshida, T., Tanabe, T., Okabe, Y., Sawasaki, T., & Chen, A. (2005). Decomposition of carbon dioxide by metals during gamma irradiation. *Radiation Research, 164*, 332–335.
37. Hiroki, A., & LaVerne, J. A. (2005). Decomposition of hydrogen peroxide at water-ceramic oxide interfaces. *The Journal of Physical Chemistry. B, 109*, 3364–3370.
38. Lien, J., Peck, K. A., Su, M. Q., & Guo, T. (2016). Sub-monolayer silver loss from large gold nanospheres detected by surface plasmon resonance in the sigmoidal region. *Journal of Colloid and Interface Science, 479*, 173–181.
39. Yoshida, T., Tanabe, T., Chen, A., Miyashita, Y., Yoshida, H., Hattori, T., & Sawasaki, T. (2003). Method for the degradation of dibutyl phthalate in water by gamma-ray irradiation. *Journal of Radioanalytical and Nuclear Chemistry, 255*, 265–269.
40. Foley, E., Carter, J., Shan, F., & Guo, T. (2005). Enhanced relaxation of nanoparticle-bound supercoiled DNA in X-ray radiation. *Chemical Communications*, 3192–3194.
41. Carter, J. D., Cheng, N. N., Qu, Y. Q., Suarez, G. D., & Guo, T. (2007). Nanoscale energy deposition by x-ray absorbing nanostructures. *The Journal of Physical Chemistry. B, 111*, 11622–11625.
42. Carter, J. D., Cheng, N. N., Qu, Y. Q., Suarez, G. D., & Guo, T. (2012). Enhanced single strand breaks of supercoiled DNA in a matrix of gold nanotubes under X-ray irradiation. *Journal of Colloid and Interface Science, 378*, 70–76.
43. McMahon, S. J., Hyland, W. B., Brun, E., Butterworth, K. T., Coulter, J. A., Douki, T., Hirst, D. G., Jain, S., Kavanagh, A. P., Krpetic, Z., et al. (2011). Energy dependence of gold nanoparticle radiosensitization in plasmid DNA. *Journal of Physical Chemistry C, 115*, 20160–20167.
44. Miller, R. D., Hofer, D., Fickes, G. N., Willson, C. G., Marinero, E., Trefonas, P., & West, R. (1986). Soluble polysilanes – An interesting new class of radiation sensitive materials. *Polymer Engineering and Science, 26*, 1129–1134.
45. Oldfield, G., Ung, T., & Mulvaney, P. (2000). Au@SnO_2 core-shell nanocapacitors. *Advanced Materials, 12*, 1519–1522.
46. Gao, X., Kang, Q. S., Yeow, J. T. W., & Barnett, R. (2010). Design and evaluation of quantum dot sensors for making superficial x-ray energy radiation measurements. *Nanotechnology, 21*, *285502*.
47. Lund, E., Gustafsson, H., Danilczuk, M., Sastry, M. D., Lund, A., Vestad, T. A., Malinen, E., Hole, E. O., & Sagstuen, E. (2005). Formates and dithionates: Sensitive EPR-dosimeter materials for radiation therapy. *Applied Radiation and Isotopes, 62*, 317–324.

48. Guidelli, E. J., Ramos, A. P., Zaniquelli, M. E. D., Nicolucci, P., & Baffa, O. (2012). Synthesis and characterization of gold/alanine nanocomposites with potential properties for medical application as radiation sensors. *ACS Applied Materials & Interfaces, 4*, 5844–5851.
49. Marques, T., Schwarcke, M., Garrido, C., Zucolotto, O. B., & Nicolucci, P. (2010). Gel dosimetry analysis of gold nanoparticle application in kilovoltage radiation therapy. *Journal of Physics: Conference Series, 250*, 012084.
50. Alqathami, M., Blencowe, A., Yeo, U. J., Doran, S. J., Qiao, G., & Geso, M. (2012). Novel multicompartment 3-dimensional radiochromic radiation dosimeters for nanoparticle-enhanced radiation therapy dosimetry. *International Journal of Radiation Oncology, Biology, Physics, 84*, E549–E555.
51. Rakowski, J. T., Laha, S. S., Snyder, M. G., Buczek, M. G., Tucker, M. A., Liu, F. C., Mao, G. Z., Hillman, Y., & Lawes, G. (2015). Measurement of gold nanofilm dose enhancement using unlaminated radiochromic film. *Medical Physics, 42*, 5937–5944.
52. Pushpavanam, K., Narayanan, E., Chang, J., Sapareto, S., & Rege, K. (2015). A colorimetric plasmonic nanosensor for dosimetry of therapeutic levels of ionizing radiation. *ACS Nano, 9*, 11540–11550.
53. Pushpavanam, K., Inamdar, S., Chang, J., Bista, T., Sapareto, S., & Rege, K. (2017). Detection of therapeutic levels of ionizing radiation using plasmonic nanosensor gels. *Advanced Functional Materials, 27*.
54. Nugroho, P., Mitomo, H., Yoshii, F., & Kume, T. (2001). Degradation of poly(L-lactic acid) by gamma-irradiation. *Polymer Degradation and Stability, 72*, 337–343.
55. Hoertz, P. G., Magnus-Aryitey, D., Gupta, V., Norton, C., Doorn, S., & Ennis, T. (2013). Photocatalytic and radiocatalytic nanomaterials for the degradation of organic species. *Radiation Physics and Chemistry, 84*, 51–58.
56. Nie, Z., Liu, K. J., Zhong, C. J., Wang, L. F., Yang, Y., Tian, Q., & Liu, Y. (2007). Enhanced radical scavenging activity by antioxidant-functionalized gold nanoparticles: A novel inspiration for development of new artificial antioxidants. *Free Radical Biology & Medicine, 43*, 1243–1254.